

Probing magnetic star-planet interaction in CARMENES targets with radio observations

L. Peña-Moñino¹, M. Pérez-Torres¹, G. Blázquez-Calero¹, J.F. Gómez¹, G. Anglada¹, J. Moldón¹, A. Alberdi¹, P.J. Amado¹, J.L. Ortiz¹

¹ Instituto de Astrofísica de Andalucía-CSIC (IAA-CSIC), Glorieta de la Astronomía s/n, E-18008 Granada, Spain

Abstract

The direct detection of auroral radio emission from planets is very challenging, and limited to Jupiter-like objects, as Earth-like exoplanets are expected to have electron-cyclotron frequencies that fall below the ionosphere cut-off. However, sub-Alfvénic interaction between an exoplanet and its host star would yield also auroral emission at frequencies of a few hundred MHz and up to the GHz regime, since the relevant magnetic field is that of host star. The detection of such radio signal would validate radio observations as a new, independent method to discover exoplanets.

We will present the results from our radio campaigns, using the uGMRT (upgraded Giant Metrewave Telescope) at band 4 (550-950 MHz), of a sample of CARMENES targets, including several Earth-like objects (such as GJ 486b and GJ 806b) and Jupiter-like objects (like GJ 436 b and GJ 1214 b). I will discuss the results obtained so far, and how they may guide future observations.

1 Motivation

The discovery of the majority of exoplanets around M dwarfs, including rocky ones, has been done using radial velocity and transit measurements. However, these methods still have limitations like, for example, the inability to study planetary magnetic fields.

This is where radio observations are unique, as it is the only way we directly obtain information regarding the magnetic field of the exoplanets (since the frequency of the emission is directly proportional to the magnetic field intensity), which would give us crucial information regarding the internal structure and composition of the planets and even help us determine their potential habitability.

Ideally, we could observe directly exoplanets from its auroral radio emission. However, Earth and super-Earth exoplanets have magnetic field strengths of up to a few Gauss, which

2 Probing magnetic star-planet interaction in CARMENES targets with radio observations

would make the resulting emission take place at frequencies below the Earth’s ionospheric cutoff of ~ 10 MHz, rendering it undetectable from Earth.

There is an alternative, which is to observe the stellar emission arising from magnetic star-planet interaction (SPI). This phenomenon takes place when the planet is close enough to the host star that it is in the sub-Alfvénic regime, i.e., when the plasma speed relative to the exoplanet, v , is smaller than the Alfvén speed at the planet position, v_A , then energy and momentum can be transported upstream back to the star by Alfvén waves. This phenomenon is analogous to the auroral radio emission in Jupiter due to its interaction with its Galilean satellites, especially Io [1].

The mechanism responsible for this emission is the electron-cyclotron maser (ECM) instability, which is a coherent mechanism yielding strong, variable, highly-polarized emission. Due to its cyclotron nature, the characteristic frequency of the emission is directly proportional to the magnetic field of the star (which is crucial when preparing observing campaigns). This emission is also periodic, with a period correlated to that of the interacting planet [2, 3].

2 CARMENES targets on uGMRT

In order to test star-planet interaction as a method for exoplanet detection, we have conducted a series of radio campaigns on a selection of promising CARMENES targets with already known exoplanets using the uGMRT (see table 1). The chosen systems are relatively close (less than 16 pc away), with relatively slow rotating stars ($P_{rot} < 30$ days) and with close-orbiting exoplanets ($P_{orb} < 7$ days). And finally, using our SPI emission model (see our relevant poster here), based on Pérez-Torres+2021 [4], we also computed if the resulting signal would be intense enough to be detected from Earth. We present here our observing campaign of GJ 486, showcasing the results from our recently submitted paper (Peña-Moñino et al. submitted). We are still carrying out the data reduction and analysis for the other systems.

Table 1: Systems observed with uGMRT.

Observed system
GJ 486
GJ 806
CD Cet
GJ 436
GJ 393
GJ 3779
GJ 1214

3 Observations and data processing

We observed GJ 486 on October 30th, November 7th, 9th, 14th, 16th, 19th and 20th 2021, and January 14th and February 22nd 2022. Our observations span almost the entire orbital phase of GJ 486 b, and spreads out over more than two full rotation periods of the star. We observed at uGMRT band 4 (550-900MHz), as we expected the emission to take place at 670 MHz for an estimated stellar magnetic of 240 G.

4 Results

We did not detect any steady radio emission above 3σ level, where σ is the rms noise of the respective image of each epoch, in any of our observing epochs, neither in Stokes I, nor in Stokes V, at the position of GJ 486. We also generated an image combining all the observing epochs, which also yielded non-detections. We also obtained the dynamic spectra for all our observing epochs, both in Stokes I and V, in order to find out if we may have missed any relatively bright but very short radio emission flares whose signal could have been washed out by averaging the data. However, we also found no detections in the spectra, confirming the lack of bursting radio emission in all of our observing epochs.

5 Discussion

We study two reasons as to why we did not detect the radio signal: (1) the radio signal being too weak to be detectable, (2) the anisotropic radio beaming pointing to a direction away from the observer due to the geometry of the system.

5.1 Constraints on the stellar wind and magnetic field of the planet

With respect to point (1), we used the emission model described in our poster to constrain some of the physical parameters of the system.

In Fig. 1 we show the predicted radio emission arising from star-planet interaction in the system, as a function of the stellar mass loss rate, \dot{M}_\odot (left and central columns), and the planetary magnetic field, B_p (right column), considering and ignoring the effect of free-free absorption (blue and orange areas in the plots, respectively). The rows correspond to coronal temperatures of 2 MK (top), 1.5 MK (middle) and 1 MK (bottom). We consider an efficiency of the conversion of Poynting flux into radio emission, ϵ , in the range of 0.2% to 1%, and a solid angle in the range from 1.64 to 3.08 sr. The horizontal dashed lines in the plots represent the detection threshold of our observations. The two plots on top of the left and central columns show the Alfvén Mach number as a function of \dot{M}_\odot .

Regarding the SPI emission as a function of the mass-loss rate, we used values ranging from $0.1\times$ up to $100\times \dot{M}_\odot$ ($\dot{M}_\odot = 2\times 10^{-14} M_\odot \text{ yr}^{-1}$). We note this entire range, the planet is always in the sub-Alfvénic regime. Hence, the planet-induced Poynting flux can be transferred to the star and be re-emitted as auroral ECM emission at radio wavelengths.

4 Probing magnetic star-planet interaction in CARMENES targets with radio observations

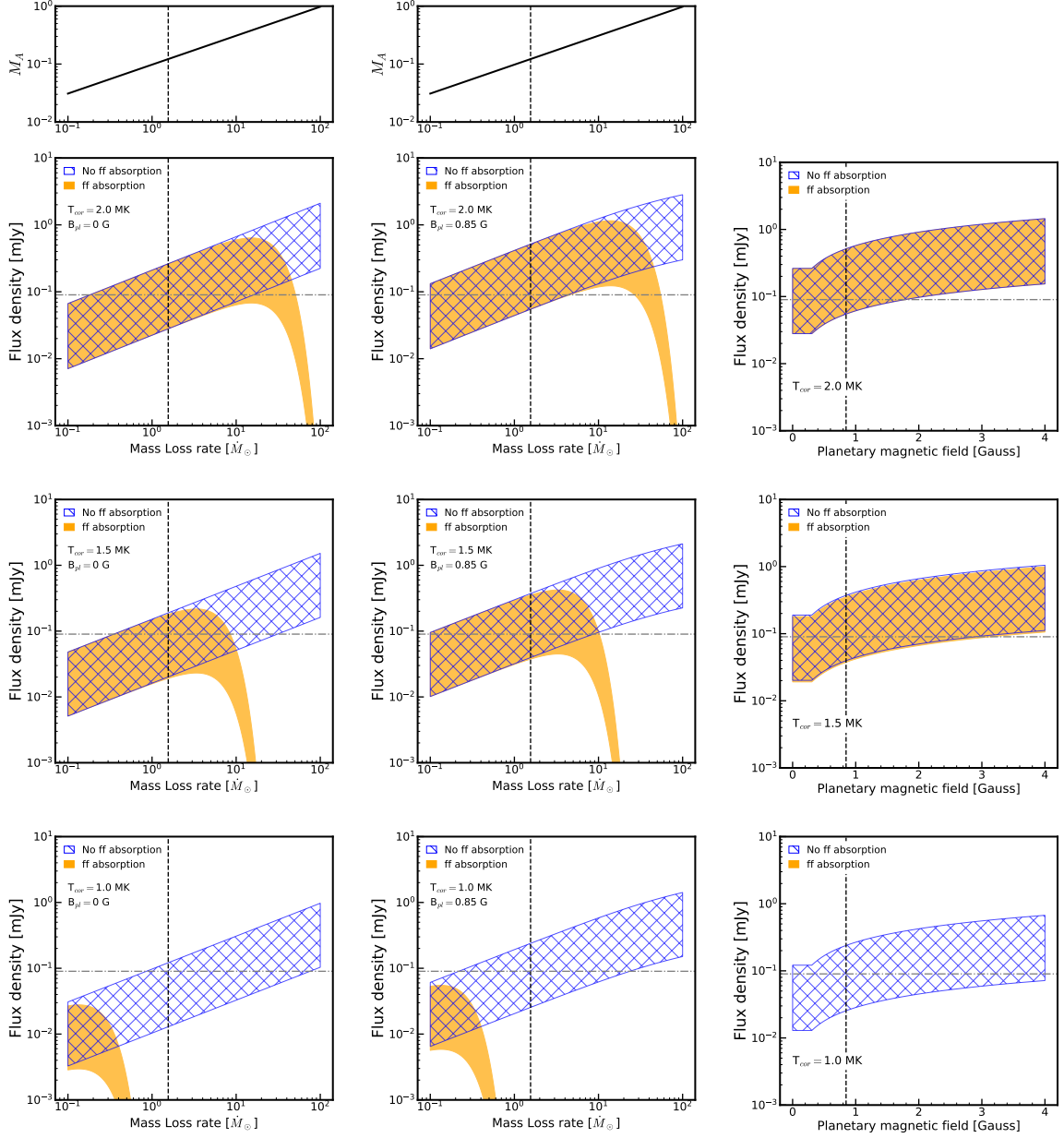


Figure 1: Predicted flux density arising at a nominal frequency of 670 MHz from star planet interaction as a function of the stellar mass-loss rate, in units of the mass-loss rate of the Sun, (left and centre columns) and as a function of the magnetic field of the planet, in Gauss (right column). The columns show the predictions for an unmagnetized (left) and a planet with a magnetic field of 0.85 G (centre). For the right panels we fix $\dot{M}_* = 1.4 \dot{M}_\odot$. The rows correspond to the expected emission for T_c values of 2, 1.5 and 1 MK (MK = MegaKelvin), respectively. The two upper panels show the Alfvén Mach number, M_A , as a function of the mass loss rate of the star. Since $\log(M_A) < 0$, the planet would fall in the sub-Alfvénic regime for the entire range of values of \dot{M}_* considered here. The predicted emission is shown for scenario with and without free-free absorption in blue and orange, respectively. Those coloured regions correspond to values of ϵ in the range from 0.002 to 0.01. The dashed line corresponds to the 3σ detection threshold of our observations (where $\sigma = 30 \mu\text{Jy b}^{-1}$).

The left panels correspond to the case of an unmagnetized planet, while the central ones to the case of a planet with $B_{pl} = 0.85$ G, the nominal magnetic field value of GJ 486b (see Appendix). The vertical lines in the plots correspond to the nominal value of $\dot{M}_* = 1.4 \dot{M}_\odot$.

The effect free-free absorption becomes more significant as the coronal temperature decreases to the point that, for the case of $T_c = 1$ MK (bottom panels), any putative SPI signal would be completely absorbed. For the nominal case of $T_c = 2$ MK, free-free absorption is already relevant for values of $\dot{M}_* > 4 \dot{M}_\odot$, independently of whether the planet is unmagnetized (left panel) or magnetized (central panel), and for $\dot{M}_* > 50 \dot{M}_\odot$, essentially all of the SPI radio emission would be absorbed by the thermal electrons in the stellar wind. If the planet is magnetized, the radio emission should have been detected if $4.6 < \dot{M}_*/\dot{M}_\odot < 27$, regardless of the assumed values of ϵ and Ω . Our non-detections therefore exclude this range of mass loss rates for the nominal value of B_{pl} . Overall, the non-detection of the radio emission suggest that the efficiency in converting Poynting flux into SPI radio emission is very low.

The right panels in Fig. 1 show the predicted SPI radio emission as a function of the planetary magnetic field, B_{pl} . The model parameters are the same ones used for the study of \dot{M}_* , except that we fixed $\dot{M}_* = 1.4\dot{M}_\odot$. If the magnetic field of the planet is >1.8 G, SPI radio emission should have been detected for $T_c = 2$ MK, even for an efficiency as small as 0.2%. For the case of $T_c = 1.0$ MK, the emission would have been completely absorbed. However, such low temperatures for the corona are unlikely to apply for M dwarfs. At any rate, our simulations illustrate the need for x-ray measurements to estimate the coronal temperatures of M dwarfs to better guide radio observations of M dwarf systems hosting exoplanets.

5.2 Constraints on the geometry of the system

It is possible that our lack of knowledge about the stellar rotation, magnetic field geometry, and/or orbital and emission cone geometry, could have resulted in the emission being beamed out of the line of sight during our observations. In order to assess that possibility, we used the MASER code developed by [5] to determine whether this was the case. MASER uses all key geometric parameters relevant for the stellar rotation, stellar magnetic field, planetary orbit, and emission cone, and determines whether radio emission generated along the magnetic field line connecting the star to the planet is visible to the observer as a function of time (called a visibility lightcurve). By creating uninformed prior distributions for each key parameter and computing the visibility lightcurve for configuration, we constructed a probability density from the sets of samples that produced lightcurves with zero visibility. If they vary with respect to the prior distributions, then those values for the parameter were more probable for the system. From our non-detections, we conclude that both the stellar inclination, i_* , and magnetic obliquity, β , must be very low, with $i_* \approx 0^\circ$ or 180° and $\beta \approx 0^\circ$ or 180° .

Acknowledgements

LPM, MPT, GB, JFG, JM, GA, AA, PA, DR, and MO acknowledge financial support through the Severo Ochoa grant CEX2021-001131-S, and through the Spanish National grants PID2020-117404GB-C21, PID2020-114461GB-I00, PID2023-146295NB-I00, all of them funded by MCIU/AEI/ 10.13039/501100011033, LPM also acknowledges funding through grant PRE2020-095421, funded by MCIU/AEI/10.13039/501100011033 and by FSE Investing in your future. We also acknowledge the service and support of the Spanish Prototype of an SRC (SPSRC), funded by the Spanish Ministry of Science, Innovation and Universities, by the Regional Government of Andalusia, by the European Regional Development Funds and by the European Union NextGenerationEU/PRTR. G.B-C acknowledges support from grant PRE2018-086111, funded by MCIN/AEI/ 10.13039/501100011033 and by 'ESF Investing in your future'

References

- [1] Zarka, P. 2007, *Planet. Space Sci.*, 55, 598
- [2] Saur, J., Grambusch, T., Duling, S., Neubauer, F. M., & Simon, S. 2013, *A&A*, 552, A119
- [3] Turnpenney, S., Nichols, J. D., Wynn, G. A., & Burleigh, M. R. 2018, *ApJ*, 854,72
- [4] Pérez-Torres, M., Gómez, J. F., Ortiz, J. L., et al. 2021, *A&A*, 645, A77
- [5] Kavanagh, R. D. & Vedantham, H. K. 2023, *MNRAS*, 524, 6267